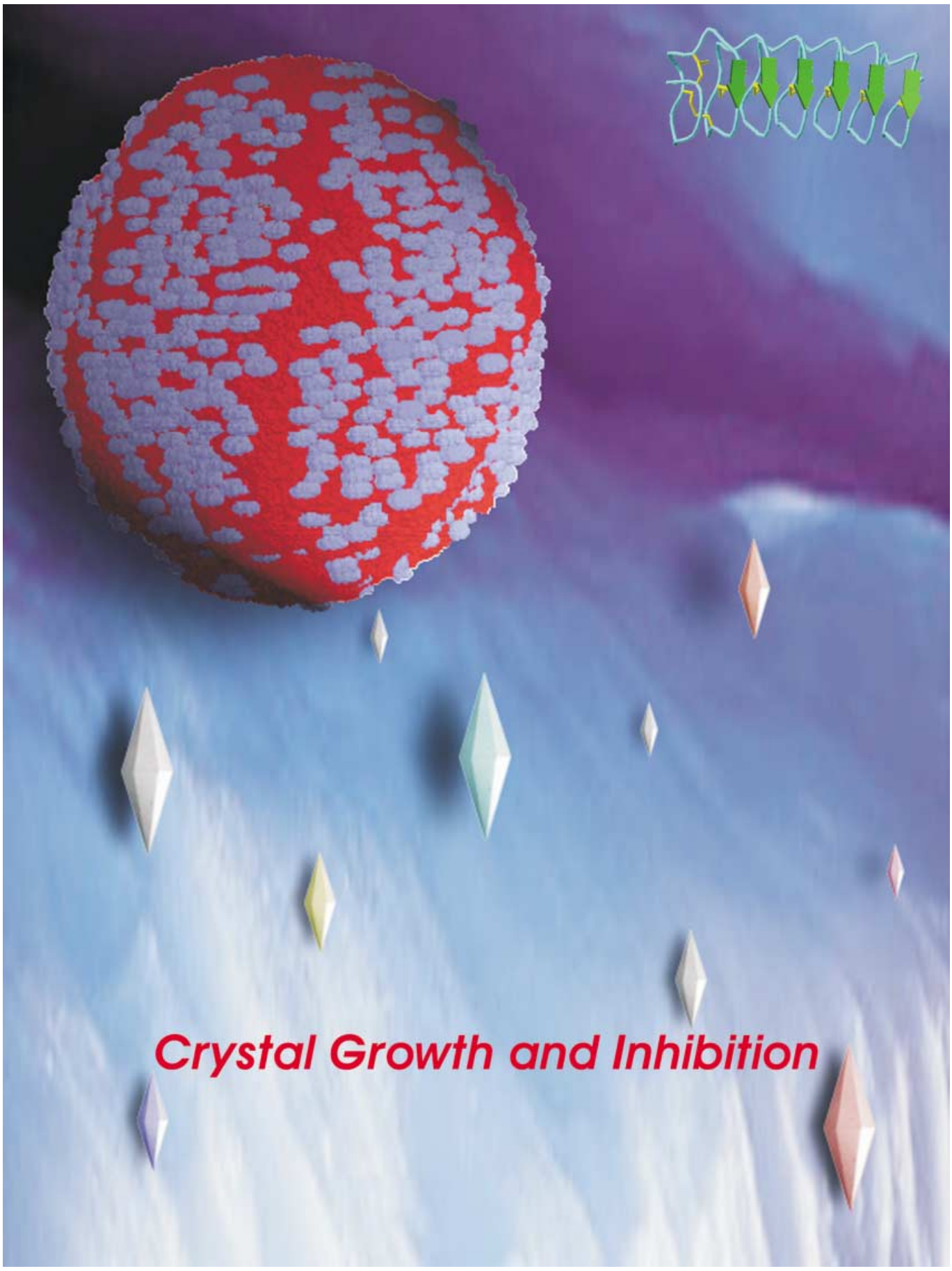

DOI: 10.1002/chem.200305186 *Chem. Eur. J.* **2004**, *10*, 1598 – 1605

New Simulation Model of Multicomponent Crystal Growth And Inhibition

Brent Wathen,[a] Michael Kuiper,[b] Virginia Walker,[b] and Zongchao Jia*[a]

Abstract: We review a novel computational model for the study of crystal structures both on their own and in conjunction with inhibitor molecules. The model advances existing Monte Carlo (MC) simulation techniques by extending them from modeling 3D crystal surface patches to modeling entire 3D crystals, and by including the use of "complex" multicomponent molecules within the simulations. These advances makes it possible to incorporate the 3D shape and non-uniform surface properties of inhibitors into simulations, and to study what effect these inhibitor properties have on the growth of whole crystals containing up to tens of millions of molecules. The application of this extended MC model to the study of antifreeze proteins (AFPs) and their effects on ice formation is reported, including the success of the technique in achieving AFP-induced ice-growth inhibition with concurrent changes to ice morphology that mimic experimental results. Simulations of ice-growth inhibition suggest that the degree of inhibition afforded by an AFP is a function of its ice-binding position relative to the underlying anisotropic growth pattern of ice. This extended MC technique is applicable to other crystal and crystal–inhibitor systems, including more complex crystal systems such as clathrates.

Keywords: ab initio calculations · antifreeze proteins · crystal growth · ice · inhibitors

Introduction

Antifreeze proteins: Antifreeze proteins (AFPs) depress the freezing point of aqueous solutions by inhibiting the growth of ice seed crystals in a noncolligative manner.[1] AFP activity, termed thermal hysteresis (TH), is defined as the difference between the resulting freezing and melting points of these solutions. The most extensively characterized AFPs come from fish that inhabit polar and other ice-laden seas, as well as from two cold-climate insects, although AFPs are also found in plants and bacteria. X-ray crystallographic and NMR studies have combined to produce high-resolution 3D structures for most of the discovered AFPs, revealing a collection that is remarkable in its structural diversity. AFP structures range from the single α-helices of type I AFP and antifreeze glycoproteins,[2,3] to the globular types II and III AFPs,[4,5] to the exceptionally regular β-helix folds in the beetle[6] and spruce budworm moth[7] AFPs (Figure 1). Several of these show striking regularities in the positioning of

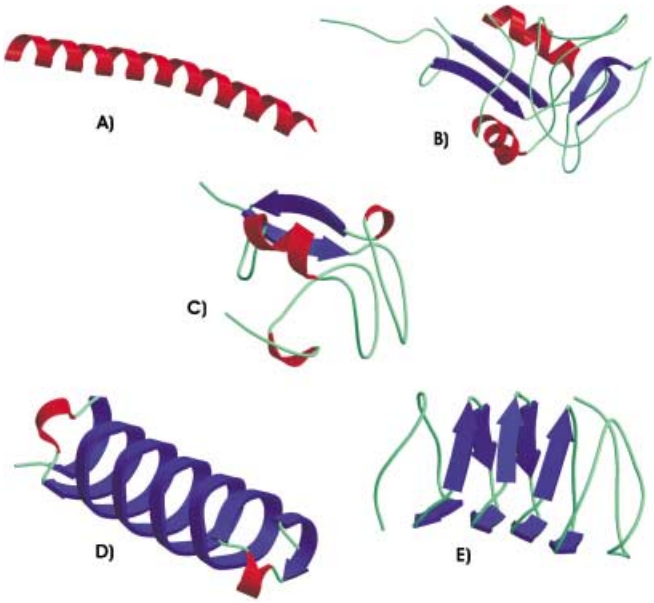

Figure 1. Representative structures for three fish AFPs (A–C) and two insect AFPs (D, E). α-Helices are shown in red, β-strands in blue, and coil region in light green. A) Type I AFP from winter flounder (PDB code: 1WFA). B) Type II AFP from sea raven (PDB code: 2AFP). C) Type III AFP from ocean pout (PDB code: 1MSI). D) Beetle AFP from *Tenebrio molitor* (PDB code: 1EZG). E) Moth AFP from spruce budworm (PDB code: 1EWW). Figures were produced using the software programs MOLSCRIPT[8] and RENDER.[9]

[a] B. Wathen, Dr. Z. Jia
Departments of Biochemistry, Queen's University
Kingston, Ontario K7L 3N6 (Canada)
Fax: (+1) 613-533-2497
E-mail: jia@post.queensu.ca

[b] Dr M. Kuiper, Dr. V. Walker
Departments of Biology, Queen's University
Kingston, Ontario K7L 3N6 (Canada)

 DOI: 10.1002/chem.200305186

suspected ice-binding motifs (for example, the recurring Thr residues in type I AFP, and the repeated Thr-X-Thr motif in the insect AFPs), while others, most notably the globular types II and III AFPs, show no obvious repetitive components on their surfaces. Indeed, these proteins appear to share little in common other than their defining characteristic of ice-growth inhibition.

Amongst AFPs, there is considerable variance in TH activity. Beetle and budworm AFPs, for example, have approximately 100 times more activity than fish AFPs on a molar basis.[6] By adsorbing to the ice surface, AFPs are thought to disrupt ice growth by introducing increased ice surface curvature, thereby altering the surface-area-to-volume ratio and making subsequent growth energetically unfavorable.[10] Unfortunately, despite the abundance of AFP structural information, the precise mechanism of this activity remains unclear. Neither X-ray crystallography nor NMR studies, both so useful for unlocking protein-.ligand interactions, are applicable for understanding AFP–ice interactions, because the AFP–ice complex is technically unsuitable for such direct studies. Thus, important questions such as what structural features differentiate an AFP from a non-AFP, or what structural features determine the maximum TH activity of an AFP, remain unanswered.

Nonbiophysical techniques, however, have been useful for the characterization of AFP–ice interactions. Ice-etching experiments pioneered by Knight et al.[11] have demonstrated that each AFP has a strong affinity for a specific plane(s) of ice. In addition, inspection of natural amino acid sequence variation and in vitro mutagenesis experiments have helped to identify AFP ice-binding faces and fostered debate on the interactive forces involved in AFP–ice interactions.[12–17] Furthermore, many in silico studies investigating AFP–ice interactions have been reported.[18–21] The majority of these have docked a single AFP to a static ice block (either with or without the presence of aqueous waters), and subjected the system to molecular dynamics and/or energy-minimization techniques. Resulting interaction energies have been used to predict optimal AFP side-chain orientations and AFP–ice docking arrangements. Two other innovative computational studies are noteworthy: a novel algorithm was used to determine the importance of protein "flatness" for AFP activity,[22] and a neural network was used to relate TH activity to fish type III AFP surface properties.[15]

In all these AFP–ice interaction studies, ice crystals are treated as static blocks. Differences in AFP activities are assumed to result from difference in AFP–ice dissociation rates related to AFP–ice binding forces and interaction energies. However, this model is problematic in three significant areas. First, an ice surface at sub-zero temperatures is a highly dynamic entity, not a static block. Second, there is a growing recognition that any TH activity requires near-irreversible AFP–ice binding due to the incredibly high association rates of water to ice at sub-zero temperatures,[1] from which it follows that differences in AFP–ice dissociation rates cannot explain difference in TH rates. Third, the focus on the binding of individual AFPs to ice surfaces has directed attention away from investigating whole-crystal phenomena, including the morphological changes that ice crystals undergo as a result of interactions with innumerable AFPs. These considerations have motivated us to re-examine the role of ice in AFP–ice interactions, seeking to understand what role ice itself may play in AFP TH activity.

Ice crystals and crystal growth theory: The common form of ice, I_h, belongs to the $P6_3/mmc$ space group and adopts an hexagonal packing arrangement that allows each constituent water molecule to form four hydrogen bonds to its nearest neighbors (Figure 2). This network of hydrogen bonds results in oriented crystal growth, whereby different surfaces of ice present specific water arrangements and hydrogen-bonding opportunities. Miller–Bravis indices, used to describe particular planes of ice, have two types of axes, three symmetrical *a* axes, and a single *c* axis.[23] Several key planes are identified by name: the basal plane (perpendicular to the *c* axis), the secondary prism plane (perpendicular to the *a* axis), and the primary prism plane (at right angles to both the basal and secondary prism planes). Of particular importance is the fact that the oriented nature of ice I_h leads to unequal growth rates, termed anisotropic growth, on different crystal surfaces. In particular, growth is much more rapid in both the primary and secondary prism plane directions than in the basal plane direction. At low degrees of

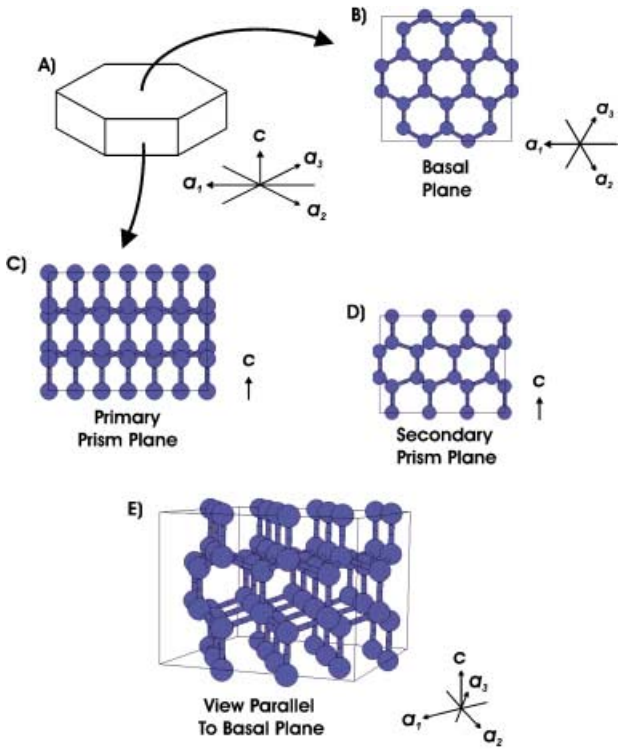

Figure 2. Views of the crystal structure of ice I_h. A) Representative diagram showing the basic repetitive hexagonal nature of ice I_h in relation to the Miller–Bravis axes system. B) Basal plane view looking down the *c* axis. C) Primary prism plane view looking perpendicular to the *c* axis. D) Secondary prism plane view, also perpendicular to the *c* axis, looking down one of the *a* axes. E) View of the ice crystal, again perpendicular to the *c* axis, this time askew from the secondary prism plane (from http://cst-www.nrl.navy.mil/lattice/).

super-cooling, this leads to ice crystals with circular disk morphologies.

As summarized by Jackson,[24] the classical expressions describing general crystal growth from the melt given by Wilson[25] and Frenkel[26] can be simplified to Equation (1):

$$\nu = \nu_0 \left[\exp\left(-\frac{L}{k_B T_E} - \frac{\sum \phi_1^i}{k_B T} \right) - \exp\left[-\frac{\sum \phi_C^i}{k_B T} \right) \right] \quad (1)$$

in which the first term describes the rate at which molecules join a crystal, and the second term describes the rate at which molecules dissociate from a crystal. Here, k_B is Boltzmann's constant, T_E is the equilibrium temperature between the solid and liquid phases, T is the absolute temperature, and the ϕs, summed over the Z's nearest neighbors of each atom at the interface, are the bond energies that are broken (ϕ_1) and formed (ϕ_C) during phase transitions. L is given by $L = (\phi_1 - \phi_C)Z/2$. Although this equation is difficult to deal with mathematically, it can be investigated by using Monte Carlo (MC) statistical simulations.[24] Unlike molecular mechanics (MM) techniques that focus on the atomic forces within and between a small number of molecules, MC statistical models forego rigorous interatomic calculations in order to model systems that contain vast numbers of molecules, enabling the study of macromolecular phenomena that result from a large number of random molecular events, such as crystal surface-growth behavior.

The basic MC technique used for crystal growth simulation is based on the kinetic Ising model.[27] Implicit in this model is an underlying lattice of spatial positions that correspond to the molecular positions inside a crystal of interest; some examples are given in Figure 3A. Gilmer identified the following assumptions underlying the kinetic Ising model:[27] 1) crystal molecules are only permitted at lattice positions, 2) only one molecule can occupy a lattice position at a time, and 3) attractive interactions between molecules only occur between nearest neighbor molecules as defined by the underlying lattice. A fourth, implicit assumption is that all participating molecules are "simple" in nature, occupying a single lattice position (Figure 3B). MC simulations proceed by maintaining a list of the occupied lattice positions, which collectively define the current shape of the crystal, and repeatedly compute, based on the probabilities described by Equation (1), whether a molecule should "join" a crystal (by occupying an interface position, defined as a vacant lattice position adjacent to an occupied lattice position) or "dissociate" from a crystal (by leaving an occupied surface lattice position, thereby rendering that position vacant). Equation (1) dictates that molecular association/dissociation probabilities are based on the number of bonds that must be formed or broken to neighboring lattice positions, and so these probabilities are *position-dependent.* However, the simplifying assumption that association probabilities are independent of position is generally adopted.[27]

Because MC statistical models for crystal growth simulation require absolute uniformity in both the crystal structure in question and in all molecular interactions, this technique has not been suitable for investigating crystal growth in which participating molecules contain structural variations

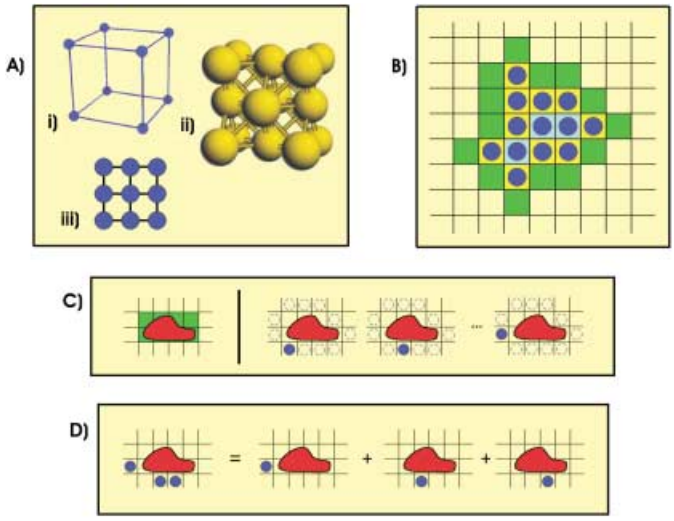

Figure 3. Monte Carlo (MC) simulations. A) Examples of lattice orientations. i) the simple cubic lattice and ii) the face centered cubic lattice. The balls represent the relative spatial lattice positions (extended repetitively in all directions), and the connecting lines define the neighboring relationship amongst positions. Also shown is iii) a simplified two-dimensional lattice, expanded in B) to illustrate a snapshot of a simulation in progress. Occupied positions are shown with a blue circle; occupied *surface* positions are in yellow, occupied *buried* positions are in cyan and vacant *interface* positions are in green. C) MC simulations using "complex" molecules. The left portion shows how the volume set for a complex molecule is defined, while the right portion shows how its energetics set is determined a priori. D) Using the predetermined energetics set, the interaction energy between a complex molecule and its neighboring crystal molecules can be determined as indicated.

or in which interaction energies amongst molecules are variable. AFPs provide an excellent example of this. While the MM techniques have been useful for understanding AFP–ice docking arrangements, whole-crystal phenomena such as ice-growth inhibition and morphological changes seem better suited to a MC approach that investigates ice crystals containing millions of water molecules interacting with hundreds or thousands of AFPs. However, AFPs are complex 3D molecules presenting non-uniform electrostatics across their surface, making them unsuitable for use in MC simulation models.

In this paper we discuss new extensions to the MC statistical model for simulating crystal growth that attempt to bridge the division between existing MC and MM modeling techniques. The application of this extended MC model to AFP ice-crystal-growth inhibition is reviewed.

Extensions to Monte Carlo Crystal Growth Simulations

Complex molecules: The MC simulation model has been extended in two fundamental ways.[28,29] The first extension enables simulations to contain molecules that occupy more than one lattice position, termed "complex" molecules. By allowing molecules to occupy more than one position, realistic 3D representations of molecules of interest (such as inhibitors) can be introduced into simulations (Figure 3C).

Furthermore, an approximation to the charge distribution on a molecular surface can be integrated into simulations by stipulating non-uniform bonding energies to neighboring lattice positions for different components of a complex molecule (Figure 3D). A molecule's 3D structure and surface properties can thus directly influence crystal growth behavior in MC simulations.

Complex molecules are incorporated into extended MC simulations by first determining a suitable crystal docking orientation(s) for the molecule, either from a known crystal structure or by performing some form of MM modeling to dock the complex molecule in question to the crystal.[28] This docking orientation is used to create the *volume set* for the molecule, which is a collection of relative 3D lattice positions that are occupied by the oriented molecule (Figure 3C). Following this, the *energetics set* for the molecule must be determined. In order for the technique to remain computationally feasible, complex molecules are limited to a finite number of fixed 3D orientations relative to the underlying lattice of crystal positions. Given this restriction, it is possible to determine approximations to the interaction energies between any two simulation molecules by using MM techniques (such as molecular dynamics or energy minimization) a priori, because molecules can only interact in a finite number of pre-determinable fixed orientations within simulations.[29] Given this a priori energetics information, the specific interaction energy between any complex molecule and a crystal structure is then defined as the sum of the interaction energies with all of its individual neighbors (Figure 3D). The *energetics set* for a complex molecule contains all precalculated interaction energies between the molecule and all other simulation molecules, in each possible relative orientation in the lattice.

Simulations involving "complex" molecules proceed in an analogous manner to those using simple molecules. As in other MC simulations, association rates are assumed to be independent of position, and thus are not determined by the energetics of bond formation. Dissociation rates are position-dependent, and so are a function of the total interaction energy between molecules and their neighbors in the lattice.

Entire 3D crystal simulations: The second extension that we have made to MC simulations is to model 3D crystals that contain up to tens of millions of simple molecules in conjunction with hundreds or thousands of complex molecules. Although existing MC techniques appear to be 3D, they are in fact only 2D because they consider only a restricted surface region, and extend the surface into the horizon by using periodic boundary conditions.[24,27,30,31] While these models can provide insights into surface properties, such as nucleation events and surface roughening, simulations of true 3D crystal structures allows for the examination of such whole-crystal phenomena as crystal morphology and inhibitor effects on crystal growth.

Whole-crystal simulations have been achieved by the judicious selection of computational storage algorithms for the crystal in the lattice. Enormous computational storage resources are required to support crystals containing up to tens of millions of molecules. To balance the requirements of mass storage and rapid access, the lattice positions in simulations are separated into *surface* positions (those lattice positions that are occupied with vacant neighboring lattice positions), *interface* positions (those lattice positions that are vacant with occupied neighboring lattice positions), and *buried* lattice positions (those occupied lattice positions that have all of their neighboring positions likewise occupied) (Figure 3B). Surface and interface lattice positions, which are the positions that participate in association and dissociation events, are contained in readily accessible lists organized by interaction energies, while buried lattice positions are maintained in a compressed format.

New MC Model Applied: Antifreeze Proteins

AFP–ice growth simulations: Out extended MC model has been applied to the study of ice crystals and ice-growth inhibition by AFPs. To model ice growth, a lattice arrangement matching the water molecule arrangement depicted in Figure 2 was adopted to properly capture the growth characteristics of ice I_h. Three AFPs were selected for use in ice growth simulations, the type I AFPs from winter flounder (WfAFP) and shorthorn sculpin (SsAFP), and the hyperactive beetle AFP from *Tenebrio molitor* (TmAFP). Docked models of each AFP bound to their ice binding planes[2,6,11,19] were obtained by using molecular dynamics and energy minimization techniques (Figure 4A). These models were used to determine the volume set for each AFP by identifying the lattice positions that are occupied by each AFP in its docked orientation. Energetic sets that describe the interaction energy between each AFP and single water molecules fixed at each possible neighboring lattice position (following Figure 3) were then determined by using energy minimization. Each AFP had a volume set composed of ~300 lattice positions, and an energetics set describing the interactions to ~400 neighboring lattice positions. Temperature-dependent association and dissociation rates were obtained for water molecules that produced crystals with circular disk morphologies. Association/dissociation rates for AFPs were empirically determined, but generally reflected the principle that AFPs with a snug fit to ice have a lower probability of dissociating than more loosely fit AFPs.

The suitability of the extended MC model was established by a comparison of the binding patterns of WfAFP and SsAFP in simulations. The results of MC simulations with both of these fish AFPs are shown in Figure 4B, and compared with experimentally derived ice etches. Although the scale between the two sets of images differs by several orders of magnitude, the similarity in binding patterns is unmistakable. To compare the differences between WfAFP and the hyperactive TmAFP, each AFP was introduced into a simulation initiated with large ice seed crystals and run at temperatures near their respective maximal TH limits.[32] For WfAFP, the seed-crystal size was 25 million water molecules and the simulation temperature was −2.0 °C; for TmAFP, the seed-crystal size was 8 million water molecules and the simulation temperature was −4.5 °C. As can be seen in Figure 5A, both AFPs were able to achieve ice-growth in-

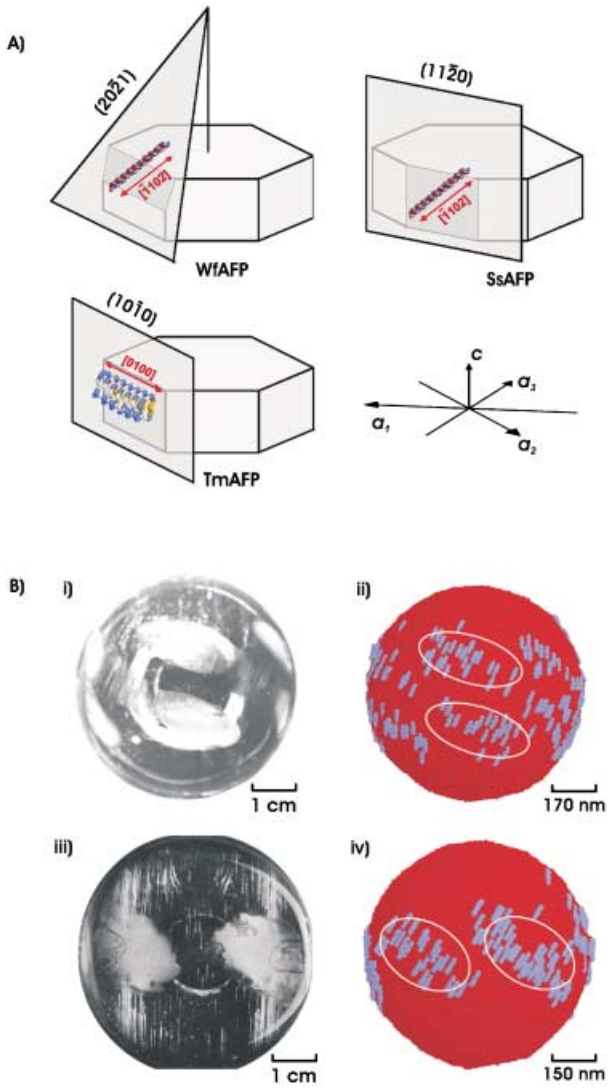

Figure 4. AFP–ice binding. A) The docking orientations used to determine volume and energetics sets for two isoforms of fish Type I AFP [isoform Hplc6 from winter flounter AFP (WfAFP) and isoform ss8 of shorthorn sculpin AFP (SsAFP)], and one insect AFP (TmAFP) are shown. B) Comparison of AFP ice-etching experiments with AFP ice-binding in simulations, using WfAFP (i/ii) and SsAFP (iii/iv). i) and iii) show the results of ice-etching experiments in which we transferred ice hemispheres to dilute solutions of AFPs ($\sim < 0.01$ mg mL^{-1}) in order to deduce preferential ice binding planes (which appear as frosted regions). ii) and iv) show the preferred binding locations for AFPs (blue cylinders) on ice crystals (red spheres). White ovals have been added to the simulated surfaces to highlight adsorption planes.

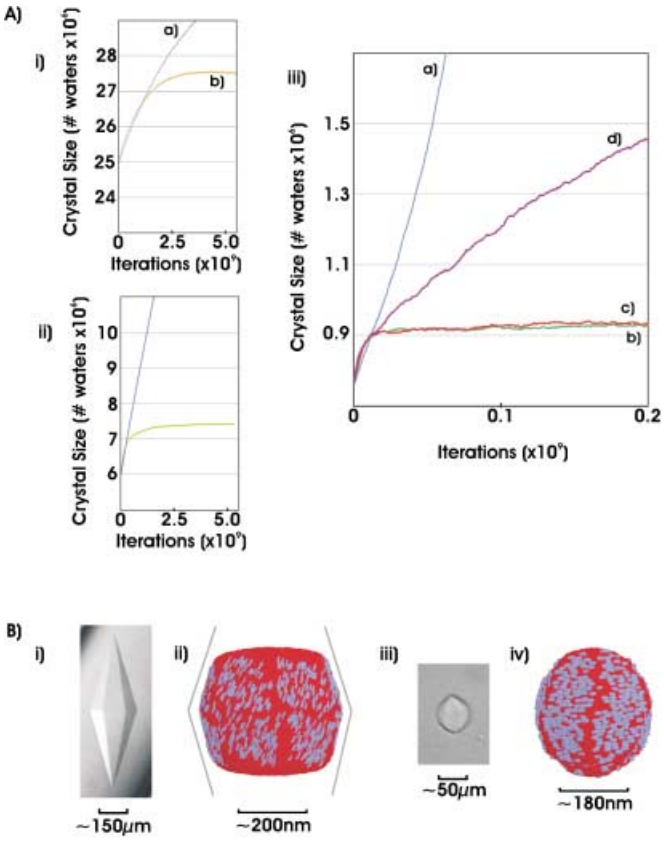

Figure 5. AFP effects on ice growth. A) Ice-growth inhibition. i) Growth of an initial seed crystal containing 25 million water molecules grown at −2.0 °C, both on its own (line a) and in the presence of WfAFP (line b). ii) Similar to i) except for 6 million water molecules at −4.5 °C with TmAFP. iii) Comparison of the AF abilities of WfAFP and TmAFP. Here, all plots show the growth of a seed crystal containing 750 000 water molecules at −3.5 °C. a) Unrestricted ice growth. b) Ice growth in the presence of TmAFP. c) Same as b), but with a doubled AFP off rate. d) Ice growth in the presence of WfAFP using the off rates from b) reduced by 80 % (increasing the binding strength of this AFP 5-fold). B) AFP-induced morphology effects. i) Hexagonal bipyramid crystal grown in vitro in the presence of WfAFP. ii) Ice morphology arising in silico after prolonged simulation time (lines added to highlight inhibited planes). iii) In vitro biconcave morphology of ice crystals grown in the presence of TmAFP. iv) Similar ice morphology arising in silico from simulations involving TmAFP.

hibition for prolonged simulation time (more than 5 billion association/dissociation events). To directly compare their ice-growth-inhibition abilities, both AFPs were also subjected to simulations starting from the same seed crystal (750 000 water molecules) and using the same simulation temperature (−3.5 °C) (Figure 5A). Mirroring the results obtained from physical experiments, TmAFP was able to inhibit ice growth under these conditions, while WfAFP could not. Furthermore, artificially increasing the dissociation rates for TmAFP by a factor of two (a net decrease in binding affinity) failed to significantly reduce its ability to inhibit crystal growth. As well, an artificial decrease in the dissociation rates for WfAFP by a factor of five (a net increase in binding affinity) likewise failed to improve its ability to inhibit ice growth. In addition, ice crystal morphologies underwent remarkable changes during the course of the simulations, mimicking the effects seen in vitro (Figure 5B). Actual crystals grown in the presence of TmAFP and WfAFP, and those obtained after prolonged simulations in the presence of these AFPs, were transformed from their initial spherical seed crystals into the characteristic hexagonal bipyramid and lemon-shaped, biconcave morphologies, respectively.[6,33]

The close-up views of ice crystal growth shown in Figure 6 illustrate the effects of AFP–ice binding on the ice-growth process. The first frame shows ordered step growth as newly nucleated layers of the prism plane grow out towards the edges. In contrast, the second frame shows a much more chaotic picture of prism growth in the presence of bound

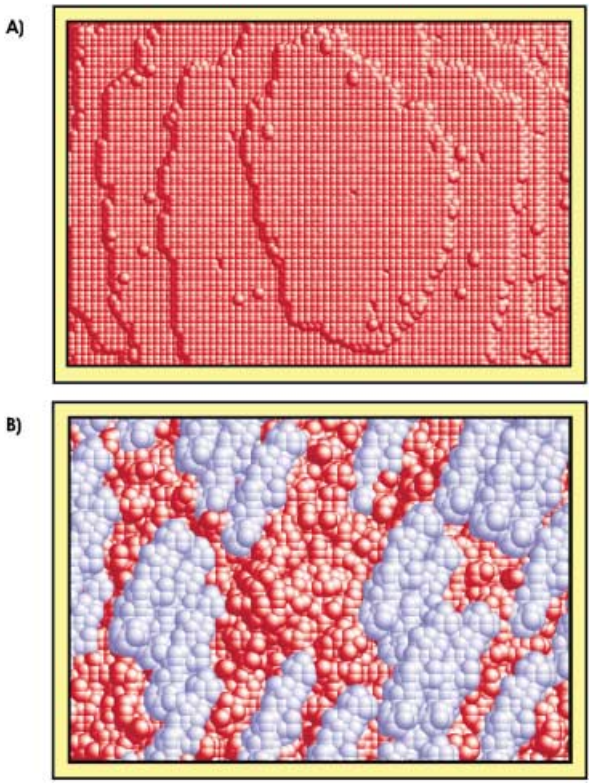

Figure 6. Prism plane growth. A) Step growth on the ice prism plane that occurs in the absence of AFPs. Several single water molecules can be seen in the figure, showing the dynamic nature of ice growth as new nucleation events are spontaneously occurring. B) Effects of AFPs on the highly regular step growth illustrated in A). Here, WfAFP, inhibiting ice growth at −2.0°C, increases the local surface curvature by forcing ice to grow in bulges between bound AFPs.

AFPs, resulting in a dramatic increase in the local surface curvature of ice. These views are consistent with current theories of both ice growth[34] and AFP-mediated ice-growth inhibition.[10]

Antifreeze protein activity—thermal hysteresis as a function of binding position: Evidence from both ice-etching[3,11] and ice-column-purification experiments,[35] coupled with the highly elevated water association rate to ice at sub-zero temperatures, suggests that AFPs must bind (essentially) irreversibly to ice regardless of their TH activity. As noted in these MC simulations, alterations to an AFP's dissociation rates (prior to achieving irreversible binding) did not alter its antifreeze abilities. These experiments and in silico findings, taken together, indicate that AFP–ice binding strength does not determine the level of TH activity.

Because ice-growth inhibition was achieved in simulations, we were able to visually examine the AFP–ice crystal system during growth inhibition. Figure 5B shows that ice surface coverage for WfAFP and TmAFP are distinct. WfAFP, which has a large *c* axis component to its binding orientation, cannot bind to the basal plane, leaving that portion of the crystal surface largely exposed. By contrast, the binding orientation of TmAFP has virtually no *c* axis component, and so, given a minimal basal surface curvature, this AFP is able to bind to the basal plane. From the examination dozens of simulation snapshots, it appears that this greater surface coverage is responsible for the improved TH activity of the beetle AFP.

WfAFP and TmAFP are both rodlike proteins with roughly equal dimensions. Were ice to grow *isotropically*, ice crystals would be spherical in nature; such crystals grown in the presence of either of these two AFPs would be expected to have the same amount of AFP–crystal coverage, though at different surface patches tangential to their binding orientations. We can conclude then, that the differences in surface coverage found for WfAFP and TmAFP are ultimately a result of their binding orientations in relation to the *anisotropic* nature of ice growth. TmAFP, with its binding orientation perpendicular to the axis of the slowest growing surface of ice, proves to be a more active AFP than WfAFP, with its binding orientation almost parallel to the axis of this slowest growing plane. Ultimately, binding orientations relative to the oriented ice crystal dictate the maximal supported surface curvatures, which themselves indicate the maximal TH activity that can be supported.

Concluding Remarks

We have extended current MC models of crystal growth to include the use of complex molecules that have 3D structures and variable surface properties. This extension allows for the inclusion of noncrystal molecules in simulations to study their structural and electrostatic effects on crystal formation. We have also extended the technique from simulating 2D surfaces to whole 3D crystals. This model has been applied to the study of AFP ice-growth inhibition, producing simulation results in good agreement with reported experimental observations. The ability to study crystal growth in molecular detail has enabled us to postulate that AFP activity relies primarily on AFP ice-binding positioning, with respect to the underlying orientation of ice, rather than from the strength of the AFP–ice interaction.

MC simulations provide an opportunity for the investigation of both crystal growth and crystal-growth inhibition by enabling a degree of control not otherwise possible. One can artificially adjust any of the following properties and compare the resulting crystals against a control crystal: association/dissociation rates for simple and complex molecules, the reversibility of complex molecule binding, the 3D structure of complex molecules, the degree of cooperation or competition amongst complex molecules, or the binding orientations of complex molecules.

Because we have designed this model to be generic, it can be applied to the study of other crystal structures or any system in which the constituent molecules are assembled in a regular fashion. We are currently applying this model to clathrates, which involve two "simple" molecules, water, and gas, each having its own association/dissociation rates and defined neighboring network. We are also interested in applying this technique to the study of nanotechnologies.

Acknowledgement

This work is supported by CIHR, NSERC and CFI/Ontario Provincial Government. Zongchao Jia is a Canada Research Chair in Structural Biology.

[1] Z. Jia, P. Davies, *Trends Biochem. Sci.* **2002**, *27*, 101.
[2] D. S. C. Yang, M. Sax, A. Chakrabartty, C. L. Hew, *Nature* **1988**, *333*, 232.
[3] C. A. Knight, E. Driggers, A. L. Devries, *Biophys. J.* **1993**, 64, 252.
[4] W. Gronwald, M. C. Loewen, B. Lix, A. J. Daugulis, F. D. Sonnichsen, P. L. Davies, B. D. Sykes, *Biochemistry* **1998**, *37*, 4712.
[5] Z. Jia, C. I. DeLuca, H. Chao, P. L. Davies, *Nature* **1996**, *384*, 285; corrigendum: Z. Jia, C. I. DeLuca, H. Chao, P. L. Davies, *Nature* **1997**, *385*, 555.
[6] Y. C. Liou, A. Tocilj, P. L. Davies, Z. Jia, *Nature* **2000**, *406*, 322.
[7] E. K. Leinala, P. L. Davies, Z. Jia, *Structure* **2002**, *10*, 619.
[8] P. J. Kraulis, *J. Appl. Crystallogr.* **1991**, *24*, 946.
[9] E. A. Merritt, D. J. Bacon, *Methods Enzymol.* **1997**, 277, 505.
[10] J. A. Raymond, A. L. Devries, *Proc. Natl. Acad. Sci. USA* **1977**, *74*, 2589.
[11] C. A. Knight, C. C. Cheng, A. L. Devries, *Biophys. J.* **1991**, 59, 409.
[12] M. M. Harding, L. G. Ward, A. D. Haymet, *Eur. J. Biochem.* **1999**, *264*, 653.
[13] J. Baardsnes, L. H. Kondejewski, R. S. Hodges, H. Chao, C. Kay, P. L. Davies, *FEBS Lett.* **1999**, *463*, 87.
[14] C. I. DeLuca, P. L. Davies, Q. Ye, Z. Jia, *J. Mol. Biol.* **1998**, *275*, 515.
[15] S. P. Graether, C. I. DeLuca, J. Baardsnes, G. A. Hill, P. L. Davies, Z. Jia, *J. Biol. Chem.* **1999**, *274*, 11842.
[16] S. P. Graether, M. J. Kuiper, S. M. Gagner, V. K. Walker, Z. Jia, B. D. Sykes, P. L. Davies, *Nature* **2000**, *406*, 325.
[17] C. B. Marshall, M. E. Delay, L. A. Graham, B. D. Sykes, P. L. Davies, *FEBS Lett.* **2002**, *529*, 261.
[18] J. D. Madura, A. Wierzbicki, J. P. Harrington, R. H. Maughon, J. A. Raymond, C. S. Sikes, *J. Am. Chem. Soc.* **1994**, *116*, 417.
[19] A. Wierzbicki, M. S. Taylor, C. A. Knight, J. D. Madura, J. P. Harrington, C. S. Sikes, *Biophys. J.* **1996**, 71, 8.
[20] J. D. Madura, K. Baran, A. Wierzbicki, *J. Mol. Recognit.* **2000**, *13*, 101.
[21] J. A. Hayward, A. D. Haymet, *J. Chem. Phys.* **2001**, *114*, 3713.
[22] D. S. Yang, W. Hon, S. Bubanko, Y. Xue, J. Seetharaman, C. L. Hew, F. Sicheri, *Biophys. J.* **1998**, 74, 2142.
[23] P. V. Hobbs, *Ice Physics*, Oxford University Press, Oxford, **1974**, p. 725.
[24] K. A. Jackson, *J. Cryst. Growth* **1999**, *198*/199, 1.
[25] H. Hertz, *Ann. Phys.* **1882**, *17*, 177.
[26] M. Knudsen, *Ann. Phys.* **1909**, *34*, 593.
[27] G. H. Gilmer, *Science* **1980**, *208*, 355.
[28] B. Wathen, M. J. Kuiper, V. K. Walker, Z. Jia, *J. Am. Chem. Soc.* **2003**, *125*, 729.
[29] B. Wathen, M. J. Kuiper, V. K. Walker and Z. Jia, *Can. J. Phys.* **2003**, *81*, 39–45.
[30] R. F. Xiao, J. I. Alexander, F. Rosenberger, *J. Cryst. Growth* **1990**, *100*, 313.
[31] E. Yokoyama, *J. Cryst. Growth* **1993**, *128*, 251.
[32] L. A. Graham, Y. C. Liou, V. K. Walker, P. L. Davies, *Nature* **1997**, *388*, 727.
[33] C. L. Hew, D. S. Yang, *Eur. J. Biochem.* **1992**, *203*, 33.
[34] P. V. Hobbs, *Ice Physics*, Oxford University Press, Oxford, **1974**, p. 556.
[35] M. J. Kuiper, C. Lankin, S. Y. Gauthier, V. K. Walker, P. L. Davies, *Biochem. Biophys. Res. Commun.* **2003**, *300*, 645.

Published online: January 29, 2004

ADDENDUM

Note added in proof (March 12, 2004): (After Early View version appeared January 29, 2004.) A recent publication has for the first time provided experimental evidence supporting the theory put forth in this paper. They conclude that the activity of AFPs is not determined by their ice-binding affinity. Partitioning of fish and insect antifreeze proteins into ice suggests they bind with comparable affinity. C. B. Marshall, M. M. Tomczak, S. Y. Gauthier, M. J. Kuiper, C. Lankin, V. K. Walker, P. L. Davies, *Biochemistry* **2004**, *43*, 148–154.

